Results and Discussion

We attempted to visualize the nucleoids of two organelles, the mitochondrion and the apicoplast, of the human malaria parasite *P. falciparum*. In this study, two highly sensitive DNA-staining dyes, SYBR Green I and PicoGreen, were tested.

First, we tested to stain *P. falciparum* 3D7 cells developing in the erythrocyte with SYBR Green I. This dye, which has an emission peak at 520 nm following excitation at 254 or 497 nm, is one of the most sensitive, commercially-available fluorochrome stains of dsDNA. The sensitivity of SYBR Green I to dsDNA is sufficient to detect DNA in a gel as low as 50 pg/ml, which is 200 times more sensitive than Hoechst dyes (Matsui *et al.* 2004). SYBR Green I is regularly used for various molecular biological experiments such as gel electrophoresis (Skeidsvoll and Ueland 1995, Zabzdyr and Lillard 2001), dsDNA quantification in solution (Vitdthum *et al.* 1999) and real-time PCR (Konnai *et al.* 2003, Ricketts *et al.* 2004). As SYBR Green I is highly-permeable but noninvasive for living cells, it has also been used for visualization of organellar nucleoids of organisms such as *Chlamydomonas reinhardtii* (Nishimura *et al.* 1998), tobacco BY-2 cells (Arimura *et al.* 2004) and *Oryzias latipes* (Nishimura *et al.* 2006).

Diluting the commercially-available stock solution between 1:100,000 and 1:1,000, we prepared a series of incubation media containing the fluorescent dye at various concentrations. When the ring-stage parasites were stained with SYBR Green I at a 1:50,000 dilution for 1 minute, there were one or two tiny, nucleoids-like bodies identified in each parasite. In the parasites observed, 86% carried only one fluorescent body (Fig. 1a) while remaining 14% had two bodies per cell. The parasite in this development stage contains one rod-shaped mitochondrion and one round apicoplast in a close proximity to each other (van Dooren *et al.* 2005, Hopkins *et al.* 1999). When the parasites were stained with a 1:5,000 dilution of SYBR Green I, the percentage of cells with two visible extra-nuclear bodies (Fig. 1b) increased to 50%, but we never observed a cell with three or more bodies. Staining in media containing SYBR Green I at a higher concentrations, i.e., those at a 1:2,000 and a 1:1,000 dilutions, resulted in emission of too bright fluorescence signals from the nucleus that hindered observation of extra-nuclear signals.

Next, we examined the staining pattern of the parasite when it was stained with another fluorochrome, PicoGreen. This fluorescent molecule shares the same molecular structure with SYBR Green I; only the difference is PicoGreen has an additional dimethylamine group at the end of the propyl chain of SYBR Green I. PicoGreen selectively binds to dsDNA and exhibits a similar fluorescence profile to that of SYBR Green I - its emission peaks at 520 nm whereas excitation at 480 nm. It is used for quantification of dsDNA in solution and allows detection of 25 pg/ml dsDNA, which is 400-fold more sensitive than Hoechst (Singer *et al.* 1997). Recently, PicoGreen was

reported to be useful for visualization of nucleoids in human mitochondria that contain only a tiny amount of DNA (Ashley *et al.* 2005).

When we incubated the parasite-containing erythrocyte in a medium containing PicoGreen at a 1:300 dilution for 1 minute, we observed no nucleoid-like fluorescent body in the malaria parasites; only the nucleus of merozoites outside the erythrocyte was stained under the same condition (data not shown). However, when we extended the incubation time to more than 30 minutes, we identified one (Fig. 1c) or two (Fig. 1d) nucleoid-like fluorescent bodies in ring-stage parasites. Although those nucleoid-like fluorescent bodies were detectable in both PicoGreen and SYBR Green I stained parasites, the former dye needed longer incubation time for stain than the latter. This is probably because erythrocyte membranes surrounding the parasite are less permeable to PicoGreen than to SYBR Green I. Probably the presence of the additional dimethylamine group makes PicoGreen more hydrophilic than SYBR Green I. The elevated hydrophilicity might cause the reduce membrane permeability of the former dye compared to the latter, resulting in weaker fluorescence emitted from DNA-containing bodies and nuclei in the parasites stained with PicoGreen

DAPI staining identified two nucleoids, which were assigned to be of the mitochondrion and the apicoplast, in each *T. gondii* cell fixed with 1% glutaraldehyde (Matsuzaki *et al.* 2001). This reminded us that each of the two fluorescent bodies detected in live *P. falciparum* cells stained with SYBR Green I or PicoGreen was the nucleoid of the parasite's mitochondrion and the apicoplast, respectively. To confirm this, we examined the subcellular location of the fluorescent bodies identified in transfectant parasites expressing an organelle-localizing DsRed (Fig. 2). We expressed the DsRed fused to the leader peptide of the mitochondrial protein Hsp60 and the apicoplast protein ACP (Sato and Wilson 2004). When only one fluorescent body was stained in the ring-stage parasite with a 1:50,000 dilution of SYBR Green I, it was always in the mitochondrion (Fig. 2a) but never in the apicoplast (Fig. 2b). When two fluorescent bodies were stained with a 1:5,000 dilution of SYBR Green I, one of the two was always localized in the apicoplast (Fig. 2c). We never observed both two bodies were localized in the mitochondrion of a ring-stage parasite. Similar observations were made when the parasite was staining with PicoGreen (data not shown). These results strongly support that each fluorescent body identified in the parasite stained with SYBR Green I or PicoGreen is the organellar nucleoid, and that both the mitochondrion and the apicoplast of a ring-stage parasite have only one nucleoid.

We found that both SYBR Green I and PicoGreen are good tools for visualizing the mitochondrial and the apicoplast nucleoids. These fluorescent dyes stained the mitochondrial nucleoid more easily than that of the apicoplast. Such preferential staining of mitochondrial nucleoids has never been reported in any plants (Nishimura *et al.* 1998, Arimura *et al.* 2004). Unlike plant plastids surrounded by only two membranes, the

apicoplast is surrounded by four membranes. Perhaps, the presence of additional membranes results in a reduced permeability of these fluorochromes into the apicoplast. It is also possible that the cationic charge of SYBR Green I and PicoGreen promotes these dyes to be accumulated preferentially in the mitochondrion (McFadden *et al.* 1999).

Organellar nucleoids are thought to be the units of genetic inheritance (Garrido *et al.* 2003, Jacobs *et al.* 2000) as well as replication and transcription of organelle genomes (Wang and Bogenhagen 2006). In *P. faclparum*, the mtDNA and the apDNA are replicated at about the same time as the nuclear genome, just before the onset of schizogony (Preiser *et al.* 1996, Smeijsters *et al.* 1994, Williamson *et al.* 2002). In the early stage of schizogony, the mitochondrion changes its morphology from the simple rod-like shape to an amorphous extended shape with many blanches (van Dooren *et al.* 2005). We observed many nucleoids in a schizont by staining with a 1:50,000 dilution of SYBR Green I and they are all localized in blanches of the mitochondrion (Fig. 2d). The schizont gives rise to daughter merozoites, each of which has one mitochondrion and one apicoplast. We observed that each mitochondrial nucleoid was segregated to the organelle of a different merozoite (data not shown). These results suggest that the organellar nucleoids are segregation units of organelle DNA even in *P. falciparum*. Our methods will be useful for cytological studies to analyze the importance of the nucleoid in each organelle of the malaria parasite.

Acknowledgements

We are grateful to Shoko Namiki for excellent technical assistance and Maiko Ono for useful discussions. This work was financially supported by a Grant-in-Aid for Creative Scientific Research (18GS0314-01 to N. S. and 18GS0314 to K. K), and the British Medical Research Council (MRC).

References

Arimura, S., Yamamoto, J., Aida, G. P., Nakazono, M., Tsutsumi, N. 2004. Frequent fusion and fission of plant mitochondria with unequal nucleoid distribution. Proc. Natl. Acad. Sci. USA 101: 7805-7808.

Ashley, N., Harris, D., Poulton, J. 2005. Detection of mitochondrial DNA depletion in living human cells using PicoGreen staining. Exptl. Cell. Res. 303: 432-446

Biagini, G. A., Fisher, N., Berry, N., Stocks, P. A., Meunier, B., Williams, D. P., Bonar-Law, R., Bray, P. G., Owen, A., O'Neill, P. M., Ward, S. A. 2008. Acridinediones: selective and potent inhibitors of the malaria parasite mitochondrial bc1 complex. Mol. Pharmacol. 73: 1347-1355.

Dahl, E. L. and Rosenthal, P. J. 2008. Apicoplast translation, transcription and genome replication: targets for antimalarial antibiotics. Trends Parasitol. 24: 279-284.

Feagin, J. E. 1994. The extrachromosomal DNAs of apicomplexan parasites. Annu. Rev. Microbiol. 48: 81-104.

Fry, M., Webb, E., Pudney, M. 1990. Effect of mitochondrial inhibitors on adenosinetriphosphate levels in *Plasmodium falciparum*. Comp. Biochem. Physiol. B. 96: 775-782.

Garrido, N., Griparic, L., Jokitalo, E., Wartiovaara, J., van der Bliek, A. M., Spelbrink, J. N. 2003. Composition and dynamics of human mitochondrial nucleoids. Mol. Biol. Cell. 14: 1583-1596.

Hopkins, J., Fowler, R., Krishna, S., Wilson, I., Mitchell, G., Bannister, L. 1999. The plastid in *Plasmodium falciparum* asexual blood stages: a three-dimensional ultrastructural analysis. Protist 150: 283-295.

Jacobs, H. T., Lehtinen, S. K., Spelbrink, J. N. 2000. No sex please, we're mitochondria: a hypothesis on the somatic unit of inheritance of mammalian mtDNA. BioEssays 22: 564-572.

Kobayashi, T., Sato, S., Takamiya, S., Komaki-Yasuda, K., Yano, K., Hirata, A., Onitsuka, I., Hata, M., Mi-ichi, F., Tanaka, T., Hase, T., Miyajima, A., Kawazu, S., Watanabe, Y., Kita, K. 2007. Mitochondria and apicoplast of *Plasmodium falciparum*: Behaviour on subcellular fractionation and the implication. Mitochondrion 7: 125-132.

Kohler, S., Delwiche, C. F., Denny, P. W., Webster, P., Wilson, R. J., Palmer, J. D., Roos DS. 1997. A plastid of probable green algal origin in apicomplexan parasites. Science 275: 1485-1489.

Konnai, S., Usui, T., Ohashi, K., Onuma, M. 2003. The rapid quantitative analysis of bovine cytokine genes by real-time RT-PCR. Vet. Micro. 92: 283-294.

Kuroiwa, T. 1982. Mitochondrial nuclei. Int. Rev. Cytol. 75: 1-59.

Matsui, K., Ishii, N., Honjo, M., Kawabata, Z. 2004. Use of the SYBR Green I fluorescent dye and a centrifugal filter device for rapid determination of dissolved DNA concentration in fresh water. Aquatic. Microbial. Ecology 36: 99-105.

Matsuzaki, M., Kikuchi, T., Kita, K., Kojima, S., Kuroiwa, T. 2001. Large amounts of apicoplast nucleoid DNA and its segregation in *Toxoplasma gondii*. Protoplasma 218: 180-191.

McFadden, G. I. 1999. Endosymbiosis and evolution of the plant cell. Curr. Opin. Plant. Biol. 2: 513-519.

Nishimura, Y., Higashiyama, T., Suzuki, L., Misumi, O., Kuroiwa, T. 1998. Active digestion of sperm mitochondrial DNA in single living sperm revealed by optical tweezers. Eur. J. Cell Biol. 77: 124-133

Nishimura, Y., Yoshinari, T., Naruse, K., Yamada, T., Sumi, K., Mitani, H., Higashiyama, T., Kuroiwa, T. 2006. Active digestion of sperm mitochondrial DNA in single living sperm revealed by optical tweezers. Proc. Natl. Acad. Sci. U S A 103: 1382-1387.

Preiser, P. R., Wilson, R. J. M., Moore, P. W., McCready, S., Hajibagheri, M. A., Blight, K. J., Strath, M., Williamson, D. H. 1996. Recombination associated with replication of malarial mitochondrial DNA. EMBO J. 15: 684-693.

Ricketts, H. J., Morgan, A. J., Spurgeon, D. J., Kille, P. 2004. Measurement of annetocin gene expression: a new reproductive biomarker in earthworm ecotoxicology. Ecotoxicol. Environ. Saf. 57: 4-10

Sato, N., Terasawa, K., Miyajima, K., Kabeya, Y. 2003. Organization, developmental dynamics, and evolution of plastid nucleoids. Int. Rev. Cytol. 232: 217-262.

Sato, S. and Wilson, R. J. M. 2004. The use of DsRED in single- and dual-color fluorescence labeling of mitochondrial and plastid organelles in *Plasmodium falciparum*. Mol. Biochem. Parasitol. 134: 175-179.

Seow, F., Sato, S., Janssen, C. S., Riehle, M. O., Mukhopadhyay, A., Phillips, R. S., Wilson, R. J., Barrett, M. P. 2005. The plastidic DNA replication enzyme complex of *Plasmodium falciparum*. Mol. Biochem. Parasitol. 141: 145-153.

Singer, V. L., Jones, L. J., Yue, S. T., Haugland, R. P. 1997. Characterization of PicoGreen reagent and development of a fluorescence-based solution assay for double-stranded DNA quantitation. Anal. Biochem. 249: 228-238.

Skeidsvoll, J. and Ueland, P. M. 1995. Analysis of double-stranded DNA by capillary electrophoresis with laser-induced fluorescence detection using the monomeric dye SYBR Green I. Anal. Biochem. 231: 359-365.

Smeijsters, L. J. J. W., Zijlstra, N. M., de Vries, E., Franssen, F. F. J., Janse, C. J., Overdulve, J. P. 1994. The effect of (S)-9-(3-hydroxy-2-phosphonylmethoxypropyl) adenine on nuclear and organellar DNA synthesis in erythrocytic schizogony in malaria. Mol. Biochem. Parasitol. 67: 115-124.

Stanway, R. R., Witt, T., Zobiak, B., Aepfelbacher, M., Heussler, V. T. 2009. GFP-targeting allows visualization of the apicoplast throughout the life cycle of live malaria parasites. Biol. Cell 101: 415-430.

Trager, W. and Jensen, J. B. 1976. Human malaria parasites in continuous culture. Science 193: 673-675.

Vaidya, A. B., Akella, R. Suplick, K. 1989. Sequences similar to genes for two mitochondrial proteins and portions of ribosomal RNA in tandemly arrayed 6-kilobase-pair DNA of a malarial parasite. Mol. Biochem. Parasitol. 35: 97-107.

Vaidya, A. B., Lashgari, M. S., Pologe, L. G., Morrisey, J. 1993. Structural features of Plasmodium cytochrome b that may underlie susceptibility to 8-aminoquinolines and hydroxynaphthoquinones. Mol. Biochem. Parasitol. 58: 33-42.

van Dooren, G. G., Marti, M., Tonkin, C. J., Stimmler, L. M., Cowman, A. F., McFadden, G. I. 2005. Development of the endoplasmic reticulum, mitochondrion and apicoplast during the asexual life cycle of *Plasmodium falciparum*. Mol. Microbiol. 57: 405-419.

Vitzthum, F., Geiger, G., Bisswanger, H., Brunner, H., Bernhagen, J. A. 1999. A quantitative fluorescence-based microplate assay for the determination of double-stranded DNA using SYBR Green I and a standard ultraviolet transilluminator gel imaging system. Anal. Biochem. 276: 59-64.

Wang, Y. and Bogenhagen, D. F. 2006. Human mitochondrial DNA nucleoids are linked to protein folding machinery and metabolic enzymes at the mitochondrial inner membrane. J. Biol. Chem. 281: 25791-25802.

Williamson, D. H., Preiser, P. R., Moore, P. W., McCready, S., Strath, M., Wilson, R. J. M. 2002. The plastid DNA of the malaria parasite *Plasmodium falciparum* is replicated by two mechanisms. Mol. Microbiol. 45: 533-542.

Wilson, R. J. M., Williamson,D. H., Preiser, P. 1994. Malaria and other Apicomplexans: the "plant" connection. Infect. Agents Dis. 3: 29-37.

—, Denny, P. W., Preiser, P. R., Rangachari, K., Roberts, K., Roy, A., Whyte, A., Strath, M., Moore, D. J., Moore, P. W., Williamson, D. H. 1996. Complete gene map of the plastid-like DNA of the malaria parasite *Plasmodium falciparum*. J. Mol. Biol. 261: 155-172.

— and Williamson, D. H. 1997. Extrachromosomal DNA in Apicomplexa. Mic. Mol. Biol. Rev. 61: 1-16.

Zabzdyr, J. L. and Lillard, S. J. 2001. UV- and visible-excited fluorescence of nuclei acids separated by capillary electrophoresis. J. Chromatogr. A. 911: 269-276.

Figure Legends

Figure 1: The nucleoid of *P. falciparum* visualized by staining with SYBR Green I or PicoGreen.

The parasite was incubated in the culture medium supplemented with SYBR Green I or PicoGreen at following dilutions: a 1:50,000 (a) or a 1:5,000 (b) dilution of SYBR Green I or a 1:300 dilution of PicoGreen (c and d). Scale bar, 2.0 μm.

Figure 2: The nucleoid visualized by staining with SYBR Green I in *P. falciparum* transfectants expressing organelle-specific markers.

Erythrocytes infected by transfectant parasites expressing either a mitochondria-localizing DsRed (a and d) or an apicoplast-localizing DsRed (b and c) were incubated in the culture medium containing a 1:50,000 (a, b, d) or a 1:5,000 (c) dilution of SYBR Green I and the position of the nucleoid (arrowhead) visualized in each parasite at the ring stage (a, b, c) or a schizont (d) was monitored using a laser scanning microscope. Scale bar, 2.0 μm.

Acta Crystallographica Section F
Structural Biology and Crystallization Communications
ISSN 1744-3091

PU5281

Crystallization and preliminary crystallographic analysis of cyanide-insensitive alternative oxidase from *Trypanosoma brucei brucei*

Kido *et al.*

Synopsis
Cyanide-insensitive alternative oxidase from *T. brucei brucei* has been purified and crystallized for X-ray structure analysis.

Keywords: alternative oxidases; membrane proteins; *Trypanosoma brucei brucei*; ascofuranone.

Queries and comments
Please supply or correct as appropriate all **bold underlined** text. In describing corrections please refer to line numbers where appropriate: these are shown in grey.

Author index
Authors' names will normally be arranged alphabetically under their family name and this is commonly their last name. Prefixes (van, de *etc.*) will only be taken into account in the alphabetization if they begin with a capital letter. Authors wishing their names to be alphabetized differently should indicate this below. **Author names may appear more than once in this list; it is not necessary to mark this correction on your proofs.**

Kido, Y.
Shiba, T.
Inaoka, D.K.
Sakamoto, K.
Nara, T.
Aoki, T.
Honma, T.
Tanaka, A.
Inoue, M.
Matsuoka, S.
Moore, A.
Harada, S.
Kita, K.

$\sigma\Sigma$

doi:10.1107/S1744309109054062

Acta Crystallographica Section F
Structural Biology and Crystallization Communications
ISSN 1744-3091

Crystallization and preliminary crystallographic analysis of cyanide-insensitive alternative oxidase from *Trypanosoma brucei brucei*

Yasutoshi Kido,[a] Tomoo Shiba,[a] Daniel Ken Inaoka,[a] Kimitoshi Sakamoto,[a] Takeshi Nara,[b] Takashi Aoki,[b] Teruki Honma,[c] Akiko Tanaka,[c] Masayuki Inoue,[d] Shigeru Matsuoka,[d] Anthony Moore,[e] Shigeharu Harada[f]* and Kiyoshi Kita[a]*

[a]Department of Biomedical Chemistry, Graduate School of Medicine, The University of Tokyo, Tokyo 113-0033, Japan, [b]Department of Molecular and Cellular Parasitology, Juntendo University School of Medicine, Tokyo 113-8421, Japan, [c]Systems and Structural Biology Center, RIKEN, Tsurumi, Yokohama 230-0045, Japan, [d]Graduate School of Pharmaceutical Sciences, The University of Tokyo, Tokyo 113-0033, Japan, [e]Biochemistry and Biomedical Sciences, School of Life Sciences, University of Sussex, Falmer, Brighton, England, and [f]Department of Applied Biology, Graduate School of Science and Technology, Kyoto Institute of Technology, Kyoto 606-8585, Japan

Correspondence e-mail: harada@kit.ac.jp, kitak@m.u-tokyo.ac.jp

Received 6 September 2009
Accepted 15 December 2009

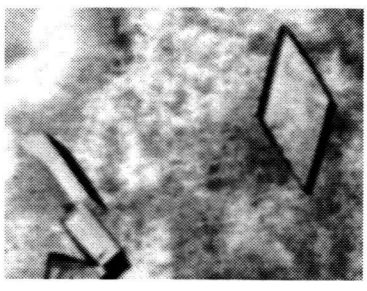

Cyanide-insensitive alternative oxidase (AOX) is a mitochondrial membrane protein and a non-proton-pumping ubiquinol oxidase that catalyzes the four-electron reduction of dioxygen to water. In the African trypanosomes, trypanosome alternative oxidase (TAO) functions as a cytochrome-independent terminal oxidase that is essential for survival in the mammalian host; hence, the enzyme is considered to be a promising drug target for the treatment of trypanosomiasis. In the present study, recombinant TAO (rTAO) overexpressed in haem-deficient *Escherichia coli* was purified and crystallized at 293 K by the hanging-drop vapour-diffusion method using polyethylene glycol 400 as a precipitant. X-ray diffraction data were collected at 100 K and were processed to 2.9 Å resolution with 93.1% completeness and an overall $R_{\rm merge}$ of 9.5%. The TAO crystals belonged to the orthorhombic space group $I222$ or $I2_12_12_1$, with unit-cell parameters $a = 63.11$, $b = 136.44$, $c = 223.06$ Å. Assuming the presence of two rTAO molecules in the asymmetric unit (2 × 38 kDa), the calculated Matthews coefficient ($V_{\rm M}$) was 3.2 Å^3 Da^{-1}, which corresponds to a solvent content of 61.0%. This is the first report of a crystal of the membrane-bound diiron proteins, which include AOXs.

1. Introduction

Cyanide-insensitive respiration in plants has been recognized since the 1920s (Moore & Siedow, 1991). Intensive biochemical studies have revealed that the mitochondrial membrane enzyme alternative oxidase (AOX) is responsible for cyanide-insensitive respiration (Moore & Siedow, 1991; Siedow & Umbach, 2000; Moore & Albury, 2008). AOX, which is cyanide-insensitive and sensitive to salicyl hydroxamic acid (SHAM), is a non-proton-pumping ubiquinol oxidase that catalyzes the four-electron reduction of dioxygen to water (Moore & Albury, 2008). AOX has been found in higher plants, algae, yeast, slime moulds, free-living amoebae, eubacteria and nematodes, as well as in protozoa, including trypanosomes (McDonald *et al.*, 2009).

Trypanosoma brucei, which causes African sleeping sickness in humans and nagana in livestock, which are serious health and economic problems in sub-Saharan Africa (World Health Organization, 2006), is known to show cyanide-insensitive respiration (Opperdoes *et al.*, 1977; Chaudhuri *et al.*, 2006). In the African trypanosomes, trypanosome alternative oxidase (TAO) functions in cyanide-insensitive respiration as a cytochrome-independent terminal oxidase (Clarkson *et al.*, 1989) that is essential for survival in the mammalian host (Clayton & Michels, 1996; Chaudhuri *et al.*, 2006).

TAO is thought to be a good target for antitrypanosomal drugs because mammalian hosts do not possess this protein (Nihei *et al.*, 2002; Chaudhuri *et al.*, 2006). Indeed, we found that ascofuranone, which is isolated from the pathogenic fungus *Ascochyta visiae*, specifically inhibits the quinol oxidase activity of TAO (Minagawa *et al.*, 1997) and rapidly kills the parasites. In addition, we have confirmed the chemotherapeutic efficacy of ascofuranone *in vivo* (Yabu *et al.*, 2003, 2006).

Although TAO and other alternative oxidases (AOXs) contain diiron-binding motifs (E*XX*H) in their amino-acid sequences, their three-dimensional structures have not yet been elucidated (Berthold

& Stenmark, 2003; Moore & Albury, 2008). The high-resolution structure of TAO will undoubtedly have considerable implications with respect to their physicochemical mechanism, enzyme reaction and structure–function relationship, including the interaction between the enzyme and ascofuranone, which may lead to the rational design of more potent and safer antitrypanosomal drugs. Here, we describe the crystallization and preliminary crystallographic analysis of TAO.

2. Materials and methods

2.1. Preparation of rTAO

To construct the host strain FN102 for the expression of rTAO, the Δ*hemA*::Km^R mutation was introduced into *Escherichia coli* strain BL21 (DE3) by P1 transduction as described in a previous study (Nihei *et al.*, 2003). The strain FN102/pTbAO (Nihei *et al.*, 2003) carrying the cDNA for *T. brucei brucei* TAO was precultured at 310 K in 100 ml LB medium (containing 10 mg ampicillin, 5 mg kanamycin and 5 mg 5-aminolevulinic acid) for 4–6 h. The precultured cells were grown aerobically at 303 K in 10 l S-medium [100 g tryptone peptone, 50 g yeast extract, 50 g casamino acids, 104 g K_2HPO_4, 30 g KH_2PO_4, 7.5 g trisodium citrate.$2H_2O$, 25 g $(NH_4)_2SO_4$, 0.5 g $MgSO_4.7H_2O$, 0.25 g $FeSO_4.7H_2O$, 0.25 g $FeCl_3$, 20 g glucose and 0.1 g carbenicillin]. The culture was started at an OD_{600} of 0.01 and expression of His_6-tagged rTAO was induced by the addition of isopropyl β-D-1-thiogalactopyranoside (IPTG; 25 μ*M*) when the OD_{600} reached 0.1. The cells were harvested 8–10 h after induction (about 40 g wet weight). The cells were then resuspended in 200 ml 50 m*M* Tris–HCl pH 7.5 containing 20%(*w*/*w*) sucrose, 0.1 m*M* phenylmethanesulfonylfluoride and Protease Inhibitor Cocktail (Sigma) and broken using a French pressure cell at 200 MPa (Ohtake, Tokyo). Unbroken cells were removed as a pellet by centrifugation at 8000*g* for 10 min (Hitachi 21G). The supernatant (35 ml) was loaded onto 35 ml 50 m*M* Tris–HCl pH 7.5 containing 40%(*w*/*w*) sucrose and ultracentrifuged at 200 000*g* for 1 h at 277 K (Hitachi 85H); the fraction of inner membranes buoyant on the 40%(*w*/*w*) sucrose layer was recovered. The inner-membrane pellet was separated by further ultracentrifugation at 200 000*g* for 1 h (Hitachi 85H) and was resuspended in 30 ml 50 m*M* Tris–HCl pH 7.5 containing 20%(*w*/*w*) sucrose. To solubilize rTAO from the membranes, the membrane suspension (35 ml) was diluted with buffer [50 m*M* Tris–HCl, 200 m*M* $MgSO_4$, 20%(*v*/*v*) glycerol pH 7.3] at 277 K to give a 6 mg ml^{-1} solution and 14%(*w*/*v*) *n*-octyl β-D-glucopyranoside (OG) was added to a final concentration of 1.4%(*w*/*v*). The solution was immediately ultracentrifuged at 200 000*g* for 1 h at 277 K to recover the supernatant containing the solubilized rTAO.

Cobalt-affinity chromatography was performed by a hybrid batch/column procedure using the manufacturer's instructions as stated below. 10 ml BD TALON Metal Affinity Resin (BD Bioscience) equilibrated in a batch format with 100 ml equilibration buffer [20 m*M* Tris–HCl, 1.4%(*w*/*v*) OG, 100 m*M* $MgSO_4$, 20%(*v*/*v*) glycerol pH 7.3] was mixed with 20 ml of the OG extract for 20 min at 277 K. The resin was washed twice with 100 ml of the first wash buffer [20 m*M* Tris–HCl, 20 m*M* imidazole, 0.042%(*w*/*v*) *n*-dodecyl β-D-maltopyranoside (DM), 50 m*M* $MgSO_4$, 20%(*v*/*v*) glycerol pH 7.3] and then transferred to a column for additional washing with 20 ml of the second wash buffer [20 m*M* Tris–HCl, 165 m*M* imidazole, 0.042%(*w*/*v*) DM, 50 m*M* $MgSO_4$, 20%(*v*/*v*) glycerol pH 7.3; flow rate 1 ml min^{-1}]. After washing, rTAO was eluted with elution buffer [20 m*M* Tris–HCl, 200 m*M* imidazole, 0.042%(*w*/*v*) DM, 50 m*M* $MgSO_4$, 60 m*M* NaCl, 20%(*v*/*v*) glycerol pH 7.3; flow rate 1 ml min^{-1}] and the fractions containing rTAO as judged by activity measurements and SDS–PAGE were pooled.

The fused N-terminal His_6 tag was removed from the purified rTAO using biotinylated thrombin and the tag-free rTAO was separated using streptavidin agarose (Biotinylated Thrombin Cleavage Capture Kit, Novagen) according to the manufacturer's instructions. Incubation with 10 U thrombin for 16 h at 293 K was required for the complete cleavage of 10 mg protein.

The molecular weight of the enzyme in solution was estimated by gel-filtration chromatography using a HiLoad 16/60 Superdex 200 pg column (GE Healthcare). Elution was carried out at a flow rate of 0.3 ml min^{-1} using 50 m*M* Tris–HCl pH 7.4, 0.1 *M* NaCl, 0.042%(*w*/*v*) DM and 20%(*v*/*v*) glycerol.

2.2. Crystallization and X-ray data collection

The purified rTAO was concentrated to 5 mg ml^{-1} in 20 m*M* Tris–HCl, 0.042%(*w*/*v*) DM, 50 m*M* $MgSO_4$, 20%(*v*/*v*) glycerol pH 7.3 using an Amicon Ultra centrifugal filter device (Millipore, 30 kDa molecular-weight cutoff) and used for initial screening of crystallization conditions. Crystallization was performed by the sitting-drop vapour-diffusion technique in 96-well Corning CrystalEX microplates with a conical flat bottom (Hampton Research). In the screening, 0.5 μl rTAO solution was mixed with an equal volume of reservoir solution and the droplet was equilibrated against 100 μl reservoir solution at 277 and 293 K. Commercially available screening kits purchased from Hampton Research (Crystal Screen, Crystal Screen II, Crystal Screen Lite, SaltRx and MembFac), Emerald BioStructures (Wizard I, Wizard II, Cryo I and Cryo II) and Fluidigm (OptiMax-5 Membrane), together with homemade grid-screen reagents containing 100 m*M* buffer (pH 5.0–9.0), 10–40%(*w*/*v*) polyethylene glycol (PEG 400, PEG 1000, PEG 3350, PEG 6000 and PEG 10 000) and 200 m*M* salts (NaCl and KCl), were used as reservoir solutions. However, crystals of rTAO did not appear.

Subsequently, screening was carried out at 277 K using various detergents (DM, OG, *n*-decyl β-D-maltopyranoside, *n*-octyl β-D-maltopyranoside, *n*-nonanoyl *N*-methyl-D-glucamine, octaethylene glycol monododecylether, tetraethylene glycol monooctylether and hexaethylene glycol monodecylether). rTAO samples dissolved in different detergents were subjected to free-interface diffusion in a TOPAZ 8.96 Screening Tip against reservoir solutions purchased from TOPAZ (OptiMax-1, OptiMax-2, OptiMax-3, OptiMax-4 PEG and OptiMax-5 Membrane) using a Fluidigm TOPAZ system (Segelke, 2005). When OG was used as a detergent, several reservoir solutions containing low-molecular-weight PEGs as precipitants gave tiny crystals. The conditions were further optimized by varying the PEG (PEG 200, PEG 400 and PEG 1000) concentration (10–40%), the buffer pH (6.0–8.0), the salt type (48 salts found in PEG/Ion Screen kit from Hampton Research) and the temperature (277 and 293 K) using the sitting-drop vapour-diffusion method. However, crystals larger than 30 μm could not be obtained and moreover they only diffracted X-rays to 7 Å resolution at most.

Next, the effects of additive detergents on crystal growth and X-ray diffraction were examined using reservoir solutions [25–40%(*w*/*v*) PEG 400, 100 m*M* imidazole buffer pH 6.2–7.8 and 200 m*M* potassium formate] supplemented with 0.1–0.5%(*w*/*v*) additive detergents. A dramatic improvement in crystal size was achieved using tetraethylene glycol monooctylether (C8E4) and the conditions, including the concentration of C8E4, were finally optimized.

Currently, crystals with average dimensions of approximately 0.1 × 0.07 × 0.03 mm can be reproducibly obtained at 293 K from reservoir solution consisting of 28–34%(*w*/*v*) PEG 400, 100 m*M* imidazole

buffer pH 7.4, 500 m*M* potassium formate and 0.4%(*w*/*v*) C8E4 using rTAO dissolved in 20 m*M* Tris–HCl pH 7.3, 0.8%(*w*/*v*) OG, 20 m*M* $MgSO_4$ and 20%(*v*/*v*) glycerol.

X-ray diffraction experiments were performed using synchrotron radiation on BL44XU and BL41XU at SPring-8 (Harima, Japan), BL5A and BL17A at Photon Factory and NW12A at Photon Factory Advanced Ring (Tsukuba, Japan). A crystal mounted in a nylon loop was frozen by rapidly submerging it in liquid nitrogen and X-ray diffraction patterns were recorded at 100 K. The best crystals diffracted X-rays to better than 3.0 Å resolution and a total of 180 images were recorded with an oscillation angle of 1°, an exposure time of 5 s per image and a crystal-to-detector distance of 280 mm. The data were processed and scaled using the *HKL*-2000 software package (Otwinowski & Minor, 1997).

3. Results and discussion

His_6-tagged rTAO was solubilized from inner membranes using OG and was purified by cobalt-affinity chromatography in the presence of DM. After removal of the fused N-terminal His_6 tag, about 10 mg of enzyme was obtained from a 10 l culture. The purified rTAO, consisting of 329 amino-acid residues (38 kDa), was >95% pure as estimated by SDS–PAGE (Fig. 1) and its molecular weight in solution was estimated to be 110 kDa by gel-filtration chromatography. As rTAO was prepared as a water-soluble rTAO–DM complex, the complex is probably composed of a homodimer of rTAO with DM molecules bound to the hydrophobic surface of the homodimer. A homodimeric structure of TAO has also been suggested by Chaudhuri *et al.* (2005). The molecular weight of the rTAO–OG complex could not be estimated because elution of rTAO from the gel-filtration column was only successful in the presence of DM as a detergent.

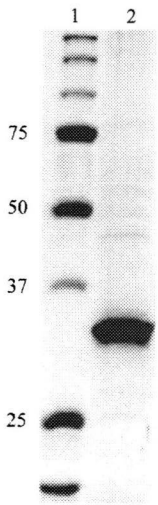

Figure 1
12.5% SDS–PAGE of rTAO with Coomassie Brilliant Blue R-250 staining. Lane 1, molecular-weight markers (kDa); lane 2, rTAO purified by affinity chromatography using BD TALON Metal Affinity Resin.

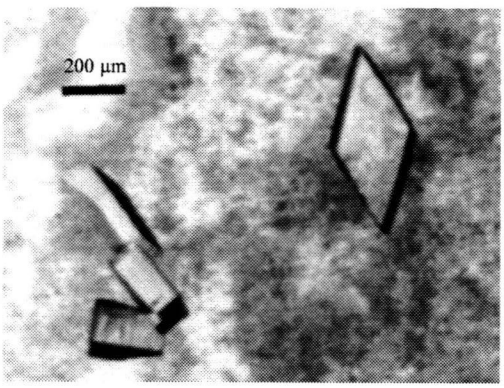

Figure 2
Rhombic plate-shaped crystals of rTAO obtained by the sitting-drop vapour-diffusion method using PEG 400 as a precipitant.

Table 1
Diffraction data statistics.

Values in parentheses are for the outermost resolution shell.

Space group	*I*222 or $I2_12_12_1$
Unit-cell parameters (Å)	a = 63.11, b = 136.44, c = 223.06
Beamline	SPring-8 BL41XU
Wavelength (Å)	1.000
Temperature (K)	100
Resolution (Å)	50.0– 2.90 (2.95–2.90)
Total reflections	135535
Unique reflections	21720
Completeness (%)	93.1 (63.2)
$R_{merge}(I)$† (%)	9.5 (57.3)
$\langle I/\sigma(I)\rangle$	9.8 (1.7)

† $R_{merge}(I) = \sum_{hkl}\sum_i |I_i(hkl) - \langle I(hkl)\rangle| / \sum_{hkl}\sum_i I_i(hkl)$, where $I_i(hkl)$ is the ith measurement of reflection hkl.

After extensive screening and optimization of crystallization conditions, crystals with average dimensions of approximately 0.1 × 0.07 × 0.03 mm could be obtained within 10 d at 293 K using rTAO dissolved in 20 m*M* Tris–HCl pH 7.3, 0.8%(*w*/*v*) OG, 20 m*M* $MgSO_4$ and 20%(*v*/*v*) glycerol with a reservoir solution containing 28–34%(*w*/*v*) PEG 400, 100 m*M* imidazole buffer pH 7.4, 100 m*M* potassium formate and 0.4%(*w*/*v*) C8E4 (Fig. 2).

Analyses of the symmetry and systematic absences in the recorded diffraction patterns indicated that the crystals belonged to the orthorhombic space group *I*222 or $I2_12_12_1$, with unit-cell parameters a = 63.11, b = 136.44, c = 223.06 Å. Assuming the presence of two rTAO molecules in the asymmetric unit (2 × 38 kDa), the calculated Matthews coefficient (V_M) is 3.2 Å^3 Da^{-1}, which corresponds to a solvent content of 61.0%. If the molecular weight of the rTAO–OG complex is presumed to be comparable to that of the rTAO–DM complex, the presence of one molecule of the rTAO–OG complex in the asymmetric unit gives a V_M value of 2.2 Å^3 Da^{-1} and a solvent content of 44.1%. A data set to 2.9 Å resolution (21 720 unique reflections) was obtained after merging 135 535 reflections recorded on 180 images, with 93.1% completeness and an overall R_{merge} of 9.5%. Statistics of data collection and processing are shown in Table 1. Currently, data collection for phasing using the anomalous dispersion effect of iron is in progress. This is the first report of the crystallization of membrane-bound diiron proteins, which include AOXs.

We thank all staff members of beamlines BL44XU and BL41XU at SPring-8, BL5A and BL17A at Photon Factory and NW12 at Photon Factory Advanced Ring for their help with X-ray diffraction data collection. This work was supported in part by grant-in-aid for Young Scientists (B) 21790402 (to YK), Creative Scientific Research Grant 18GS0314 (to KK), grant-in-aid for Scientific Research on Priority Areas 18073004 (to KK) from the Japanese Society for the Promotion of Science and the Targeted Proteins Research Program (to KK) of the Japanese Ministry of Education, Science, Culture, Sports and Technology (MEXT). ALM gratefully acknowledges the BBSRC for

financial support and, together with KK, the Prime Minister's Initiative 2 (Connect) fund for collaborative twinning.

References

Berthold, D. A. & Stenmark, P. (2003). *Annu. Rev. Plant Biol.* **54**, 497–517.

Chaudhuri, M., Ott, R. D. & Hill, G. C. (2006). *Trends Parasitol.* **22**, 484–491.

Chaudhuri, M., Ott, R. D., Saha, L., Williams, S. & Hill, G. C. (2005). *Parasitol. Res.* **96**, 178–183.

Clarkson, A. B. Jr, Bienen, E. J., Pollakis, G. & Grady, R. W. (1989). *J. Biol. Chem.* **264**, 17770–17776.

Clayton, C. E. & Michels, P. (1996). *Parasitol. Today*, **12**, 465–471.

McDonald, A. E., Vanlerberghe, G. C. & Staples, J. F. (2009). *J. Exp. Biol.* **212**, 2627–2634.

Minagawa, N., Yabu, Y., Kita, K., Nagai, K., Ohta, N., Meguro, K., Sakajo, S. & Yoshimoto, A. (1997). *Mol. Biochem. Parasitol.* **84**, 271–280.

Moore, A. L. & Albury, M. S. (2008). *Biochem. Soc. Trans.* **36**, 1022–1026.

Moore, A. L. & Siedow, J. N. (1991). *Biochim. Biophys. Acta*, **1059**, 121–140.

Nihei, C., Fukai, Y., Kawai, K., Osanai, A., Yabu, Y., Suzuki, T., Ohta, N., Minagawa, N., Nagai, K. & Kita, K. (2003). *FEBS Lett.* **538**, 35–40.

Nihei, C., Fukai, Y. & Kita, K. (2002). *Biochim. Biophys. Acta*, **1587**, 234–239.

Opperdoes, F. R., Borst, P., Bakker, S. & Leene, W. (1977). *Eur. J. Biochem.* **76**, 29–39.

Otwinowski, Z. & Minor, W. (1997). *Methods Enzymol.* **276**, 307–326.

Segelke, B. (2005). *Expert Rev. Proteomics*, **2**, 165–172.

Siedow, J. N. & Umbach, A. L. (2000). *Biochim. Biophys. Acta*, **1459**, 432–439.

World Health Organization (2006). *Wkly Epidemiol. Rec.* **81**, 71–80.

Yabu, Y., Suzuki, T., Nihei, C., Minagawa, N., Hosokawa, T., Nagai, K., Kita, K. & Ohta, N. (2006). *Parasitol. Int.* **55**, 39–43.

Yabu, Y., Yoshida, A., Suzuki, T., Nihei, C., Kawai, K., Minagawa, N., Hosokawa, T., Nagai, K., Kita, K. & Ohta, N. (2003). *Parasitol. Int.* **52**, 155–164.

Divergence of the mitochondrial genome structure in the genera *Babesia* and *Theileria*, parasites in Apicomplexa

(Research Article)

Kenji Hikosaka[1], Yoh-ichi Watanabe[2], Naotoshi Tsuji[3], Kiyoshi Kita[2], Hiroe Kishine[4], Nobuko Arisue[5], Nirianne Marie Q. Palacpac[5], Shin-ichiro Kawazu[6], Hiromi Sawai[1], Toshihiro Horii[5], Ikuo Igarashi[6], Kazuyuki Tanabe[1]*

[1]Laboratory of Malariology, International Research Center of Infectious Diseases, Research Institute for Microbial Diseases, Osaka University, Suita, Osaka, Japan

[2] Department of Biomedical Chemistry, Graduate School of Medicine, The University of Tokyo, Bunkyo-ku, Tokyo, Japan

[3]Laboratory of Parasitic Diseases, National Institute of Animal Health, National Agriculture and Food Research Organization, Tsukuba, Ibaraki, Japan

[4]Department of Molecular Biology, Research Institute for Microbial Diseases, Osaka University, Suita, Osaka, Japan

[5]Department of Molecular Protozoology, Research Institute for Microbial Diseases, Osaka University, Suita, Osaka, Japan

[6]National Research Center for Protozoan Diseases, Obihiro University of Agriculture and Veterinary Medicine, Obihiro, Hokkaido, Japan

*Author for Correspondence:

Kazuyuki Tanabe

Laboratory of Malariology, International Research Center of Infectious Diseases, Research Institute for Microbial Diseases, Osaka University, 3-1 Yamadaoka, Suita, Osaka 565-0871,

Japan.

Telephone number; +81-6-6879-4260

Fax number; +81-6-6879-4262

e-mail address; kztanabe@biken.osaka-u.ac.jp

Keywords

Mitochondrion, Mitochondrial genome; *Babesia*; *Theileria*; *Plasmodium*; Apicomplexa

Running head

Mitochondrial genomes of *Babesia* and *Theileria*

Abstract

Mitochondrial (mt) genomes from diverse phylogenetic groups vary considerably in size, structure and organization. The genus *Plasmodium*, causative agent of malaria, of the phylum Apicomplexa, has the smallest mt genome in the form of a circular and/or tandemly repeated, linear element of 6 kb, encoding only three protein genes (*cox1*, *cox3* and *cob*). The closely related genera *Babesia* and *Theileria* also have small mt genomes (6.6 kb), that are monomeric linear with an organization distinct from *Plasmodium*. To elucidate the structural divergence and evolution of mt genomes between *Babesia/Theileria* and *Plasmodium*, we determined five new sequences from *Babesia bigemina*, *B. caballi*, *B. gibsoni*, *Theileria orientalis* and *T. equi*. Together with previously reported sequences of *B. bovis*, *T. annulata* and *T. parva*, all eight *Babesia* and *Theileria* mt genomes are linear molecules with terminal inverted repeats (TIRs) on both ends, containing three protein coding genes (*cox1*, *cox3* and *cob*) and six large subunit (LSU) rRNA gene fragments. The organization and transcriptional direction of protein coding genes and the rRNA gene fragments were completely conserved in the four *Babesia* species. In contrast, notable variation occurred in the four *Theileria* species. While the genome structures of *T. annulata* and *T. parva* were nearly identical to those of *Babesia*, an inversion in the 3-kb central region was found in *T. orientalis*. Moreover, the *T. equi* mt genome is the largest (8.2 kb) and most divergent with unusually long TIR sequences, in which *cox3* and two LSU rRNA gene fragments are located. The *T. equi* mt genome showed little synteny to the other species. These results suggest that the *Theileria* mt genome is highly diverse with lineage specific evolution in two *Theileria* species: genome inversion in *T. orientalis*, and gene-embedded long TIR in *T. equi*.

Introduction

Mitochondria, organelles essential for energy transduction and cellular functions, are present in almost all eukaryotes. Like nuclear genomes of eukaryotes, mitochondrial (mt) genomes from diverse phylogenetic groups vary considerably in size, structure, and organization as well as the number of genes (Gray, Lang, and Burger 2004). The largest mt genome is found in land plants, in which the size ranges from 180 to 2,400 kb (Ward, Anderson, and Bendich 1981; Palmer, Soltis, and Soltis 1992) and the smallest is the 6-kb genome of the genus *Plasmodium*, causative agents of malaria. *Plasmodium* belongs to the phylum Apicomplexa, which includes >5,000 species, all of which are parasites of clinical or economic importance (Levine 1988). Veterinary and opportunistic pathogens includes *Babesia*, which causes babesiosis in ruminants and humans; *Theileria*, causal agents for tropical theileriosis and East Coast fever in cattle; *Cryptosporidium*, responsible for cryptosporidiosis in humans and animals; and *Toxoplasma*, causing toxoplasmosis in immunocompromised patients and congenitally infected fetuses.

Relatively few apicomplexan mt genomes have been studied and available data suggest that they are remarkably diverse in structure and genome organization. In *Plasmodium*, the mt genome is in the form of a circular and/or tandemly repeated, predominantly linear 6-kb element (Preiser et al. 1996; Wilson and Williamson 1997). The 6-kb element encodes only three mt protein coding genes (cytochrome *c* oxidase subunits I and III: *cox1* and *cox3*, and cytochrome *b*: *cob*) in addition to large subunit (LSU) and small subunit (SSU) rRNAs. The two rRNA genes are extensively fragmented and rearranged with 20 identified rRNA pieces, and curiously no tRNA genes have yet been identified (Feagin et al. 1997). The mt genomes of closely related Apicomplexa parasites *Babesia* and *Theileria* (Lau 2009) are 6.6 kb in size and monomeric linear molecules with terminal inverted repeats (TIR), indicative of telomeres (Kairo et al. 1994; Brayton et al. 2007). Similar to *Plasmodium*, mt genomes of *Babesia* and *Theileria* contain the three protein coding genes, but gene order and transcriptional direction

are clearly different from *Plasmodium* (Kairo et al. 1994; Brayton et al. 2007). Thus, the mt genomes of *Plasmodium* and *Babesia/Theileria* are structurally highly divergent regardless of their close relatedness (Kuo, Wares, and Kissinger 2008). For *Toxoplasma gondii*, the mt genome remains to be isolated and analyzed, although multiple copies of partial mt genes (*cox1* and *cob*) were found to be scattered throughout the nuclear genome (Ossorio, Sibley, and Boothroyd 1991). In *Cryptosporidum parvum*, the mitochondrion is degenerative and lacks any DNA (Abrahamsen et al. 2004). Clearly the phylum Apicomplexa, thus, provides interesting materials to further understand the evolution of mt genome.

It remains unknown how a remarkable structural divergence between *Plasmodium* and *Babesia/Theileria* as mentioned above was generated. Gathering enough dataset will also help provide further insights on the extent at which the mt genomes have evolved in the different genera as well as in the Phylum. In this study, we determined five new mt genome sequences from *Babesia* and *Theileria* species. Analyses of the genome structures show that while the mt genome structure is conserved in *Babesia* species, it notably varies in both size and genome organization in *Theileria* species, with lineage specific evolution in two *Theileria* species: genome inversion in *T. orientalis*, and gene-embedded long TIR in *T. equi*.

Materials and Methods

Parasite Species

Mitochondrial genome sequences were determined from the following seven parasite species: *Babesia bigemina* (Kochinda stock) (Fujinaga, Minami, and Ishihara 1980), *B. caballi* (USDA strain) (Avarzed et al. 1997), *B. gibsoni* (NRCPD strain) (Ishimine et al. 1978), *B. bovis* (Miyama stock) (Fujinaga, Minami, and Ishihara 1980), *Theileria orientalis* (Ikeda stock) (Kim et al. 2004), *T. equi* (USDA strain) (Avarzed et al. 1998), and *T. parva* (Muguga stock) (Kairo et al. 1994). Their host animals are cattle for *B. bigemina*, *B. bovis*, *T. orientalis*,

and *T. parva*; horses for *B. cabali* and *T. equi*; and dogs for *B. gibsoni* (supplementary table 1, Supplementary Material online).

DNA Sequencing

Parasite genomic DNA was extracted from animal bloods infected with *B. bigemina*, *B. gibsoni*, *B. bovis*, *T. orientalis* and *T. parva*, and from cultures of *B. caballi* and *T. equi*, using QIAamp DNA Blood Mini Kit (QIAGEN, Hilden, Germany) according to the manufacturer's instructions. Nucleotide sequences of the mt genomes were determined by direct sequencing of PCR products using specific primers (supplementary Table 2a, Supplementary Material online). The primers were designed by aligning reported mt genome sequences of *B. bovis* (DDBL/EMBL/GenBank accession # EU075182), *T. parva* (Z23263) and *T. annulata* (NW_001091933). Amplification was carried out in a 20 μl reaction mixture containing 0.2 μM each of forward and reverse primers, 400 μM each of dNTP, 1 unit of LA-Taq (Takara, Shiga, Japan), 2 μl of 10×PCR buffer, 2.5 mM of $MgCl_2$, and 1 μl of genomic DNA. PCR conditions were as follows: initial denaturation at 94 °C for 1 min, and amplification for 40 cycles at 94 °C for 30 s, 55-68 °C (depending on primers used) for 30 s, and 72 °C for 1-6 min (depending on amplicon size, 1 minute per kb), followed by a final extension at 72 °C for 10 min.

Sequences of the *T. equi* mt telomeric regions were determined by using the terminal deoxynucleotidyl transferase (TdT) tailing method (Bah et al. 2004) with some modifications. Briefly, the 3′-end was tailed with cytosine by initial denaturation of genomic DNA (150 ng) for 5 min at 95°C, and then incubated for 30 min at 37 °C in a reaction mixture containing 200 μM dCTP, 1 U of TdT (Takara), 20 mM Tris-HCl (pH 8.4), 50 mM KCl, and 1.5 mM $MgCl_2$; followed by heat-inactivation of TdT at 65°C for 10 min. The first PCR was done in a 50 μl reaction mixture containing 2 μl of the tailed DNA fragments, 1.25 units of AmpliTaq DNA Polymerase (Applied Biosystems, Foster City, CA), 2.5 mM $MgCl_2$, 200 μM dNTPs,

0.4 μM of a mt genome-specific primer (supplementary table 2b, Supplementary Material online) and a selective anchor primer (5′-CTACTACTACTAGGCCACGCGTCGACTAGTACGGGGGGGGGGGGGGG-3′). Initial denaturation was at 95°C for 2 min, followed by 40 cycles of 94°C for 30 s, 62°C for 3 min, with a final extension step at 72°C for 10 min. The second PCR was performed using 1 μl of the first PCR product in a 50 μl reaction mixture mentioned above, containing a nested primer (supplementary table 2b, Supplementary Material online) and a universal amplification primer (5′-CTACTACTACTAGGCCACGCGTCGACTAGTAC-3′). Nested PCR amplification was at 95°C for 2 min, and 25 cycles of 94°C for 30 s, 62°C for 2 min, followed by an extension step at 72°C for 10 min. This method could not work for the other *Babesia* and *Theileria* samples. It can be surmised that relatively high (A+T) content in TIRs of the other samples may have caused some problems. Multiple palindromes in TIR reported for *T. parva* (Shukla and Nene 1998) may also be contributing factors in the difficulty to determine telomeric sequences. In *T. equi*, unlike other *Babesia* and *Theileria* species, the TIR has a relatively low (A+T) content with no apparent multiple palindromes, and surprisingly, contains *cox3* and two fragments of rRNA gene (see Results).

TIR sequences of other *Babesia* and *Theileria* species were determined using an "inverted PCR", in which primers leading toward telomere ends (supplementary table 2b, Supplementary Material online) were used. We assumed that small inverted sequences, probably present in TIRs as reported for *T. parva* (Shukla and Nene 1998), could self-anneal in opposite direction, enabling amplification of two telomeric regions encompassed by two outward primers when *Taq* polymerase with an exonuclease activity, that could excise unpaired bases (such as LA-Taq), was used. This "inverted PCR" successfully amplified specific DNA bands for all (*Babesia* and *Theileria)* but one species (*i.e*, *T. equi*) examined here.

PCR products were purified using QIAquick PCR purification kit (QIAGEN). DNA

sequencing was performed directly from two independent PCR products, using the BigDye® Terminator v3.1 Cycle Sequencing Kit (Applied Biosystems) and an ABI 3130 Genetic Analyzer (Applied Biosystems). Sequencing primers were designed to cover target regions in both directions. DDBL/EMBL/GenBank accession numbers of sequences obtained in this study are given in supplementary table 1 (Supplementary Material online). The *T. parva* sequence obtained here has a 24 bp inconsistency with the reported *T. parva* sequence (Z23263). The *B. bovis* sequence in this study has a 7-bp difference from the reported *B. bovis* sequence (EU075182). These differences may be due to polymorphism, because uncloned stock (*T. parva*) and different parasite strains (*B. bovis*) were used. We used our sequences of *T. parva* and *B. bovis* for analysis.

Gene Annotation

Nucleotide sequences of obtained mt genomes from *Babesia* and *Theileria* species and their deduced amino acid sequences were aligned together with reported sequences from *B. bovis* (EU075182), *T. parva* (Z23263) and *T. annulata* (NW_001091933) by CLUSTAL W (Thompson, Higgins, and Gibson 1994). Alignment was manually corrected. Protein-coding genes were predicted using previously annotated sequences from *T. parva* and *B. bovis*.

To identify putative rRNA genes, mt DNA sequences or annotated rRNA gene fragments from *B. bovis* (EU075182) and *T. parva* (Z23263) was used as query under the suggested algorithm parameters (Freyhult, Bollback, and Gardner 2007) in NCBI BLAST 2.2 (Altschul et al. 1990). In silico analysis was also done with Probalign beta version 1.2 (Roshan, Chikkagoudar, and Livesay 2008) and SSEARCH 3.5 (Pearson 1991) using known rRNA gene fragments and suggested advanced search options (Freyhult, Bollback, and Gardner 2007; Roshan, Chikkagoudar, and Livesay 2008). Newly identified candidate rRNA genes were, likewise, used as input sequences. The information from sequence alignments using CLUSTAL W (Thompson, Higgins, and Gibson 1994) and putative base-pairings